






AdipoR agonist increases insulin sensitivity and exercise endurance in AdipoR-humanized mice

Masato Iwabu^{1,2,3,11}, Miki Okada-Iwabu ^{1,3,11}✉, Hiroaki Tanabe ^{4,5}, Nozomi Ohuchi¹, Keiko Miyata¹, Toshiko Kobori⁶, Sara Odawara¹, Yuri Kadowaki¹, Shigeyuki Yokoyama ^{4,5}, Toshimasa Yamauchi ^{1,7}✉ & Takashi Kadowaki ^{1,8,9,10}✉

Adiponectin receptors, AdipoR1 and AdipoR2 exert anti-diabetic effects. Although muscle-specific disruption of AdipoR1 has been shown to result in decreased insulin sensitivity and decreased exercise endurance, it remains to be determined whether upregulation of AdipoR1 could reverse them in obese diabetic mice. Here, we show that muscle-specific expression of human AdipoR1 increased expression levels of genes involved in mitochondrial biogenesis and oxidative stress-detoxification to almost the same extents as treadmill exercise, and concomitantly increased insulin sensitivity and exercise endurance in obese diabetic mice. Moreover, we created AdipoR-humanized mice which express human AdipoR1 in muscle of AdipoR1-R2 double-knockout mice. Most importantly, the small-molecule AdipoR agonist AdipoRon could exert its beneficial effects in muscle via human AdipoR, and increased insulin sensitivity and exercise endurance in AdipoR-humanized mice. This study suggests that expression of human AdipoR1 in skeletal muscle could be exercise-mimetics, and that AdipoRon could exert its beneficial effects via human AdipoR1.

¹Department of Diabetes and Metabolic Diseases, Graduate School of Medicine, The University of Tokyo, 7-3-1 Hongo, Bunkyo-ku, Tokyo 113-0033, Japan. ²PRESTO, Japan Science and Technology Agency, 4-1-8 Honcho, Kawaguchi, Saitama 332-0012, Japan. ³Laboratory for Advanced Research on Pathophysiology of Metabolic Diseases, The University of Tokyo, 7-3-1 Hongo, Bunkyo-ku, Tokyo 113-0033, Japan. ⁴RIKEN Structural Biology Laboratory, 1-7-22 Suehiro-cho, Tsurumi-ku, Yokohama 230-0045, Japan. ⁵RIKEN Cluster for Science, Technology and Innovation Hub, 1-7-22 Suehiro-cho, Tsurumi-ku, Yokohama 230-0045, Japan. ⁶Division of Diabetes and Metabolism, The Institute for Adult Diseases, Asahi Life Foundation, 2-2-6 Nihonbashibakuro-cho, Chuo-ku, Tokyo 103-0002, Japan. ⁷AMED-CREST, Japan Agency for Medical Research and Development, 1-7-1 Otemachi, Chiyoda-ku, Tokyo 100-0004, Japan. ⁸Department of Prevention of Diabetes and Life-style Related Diseases, The University of Tokyo, 7-3-1 Hongo, Bunkyo-ku, Tokyo 113-0033, Japan. ⁹Department of Metabolism and Nutrition, Mizonokuchi Hospital, Faculty of Medicine, Teikyo University, 5-1-1 Futago, Takatsu-ku, Kawasaki, Kanagawa 213-8507, Japan. ¹⁰Toranomon hospital, 2-2-2 Toranomon, Minato-ku, Tokyo 105-8470, Japan. ¹¹These authors contributed equally: Masato Iwabu, Miki Okada-Iwabu. ✉email: omiki-tyk@umin.ac.jp; tyamau-tyk@umin.ac.jp; t-kadowaki@toranomon.kkr.or.jp

Lack of exercise¹ associated with increasing societal automation, as well as changes in dietary habits, has led to a drastic increase in the number of overweight individuals worldwide^{2,3}. Obesity is known to cause insulin resistance, which is associated with type 2 diabetes and cardiovascular disease^{4–6}, where it has become clear that decreased plasma adiponectin levels in obesity are causally implicated in these obesity-linked diseases^{7–9}.

Adiponectin^{10–13} is a secreted protein highly expressed specifically in adipose tissue known as an adipokine^{14–16}. Adiponectin, a member of the C1q/TNF related protein (CTRP) family that includes at least 15 other members (CTRP1–15) including some shown to regulate metabolism, has attracted much interest because of its anti-inflammatory and insulin-sensitizing effects¹⁷. Plasma levels of adiponectin have been shown to be decreased in obesity, insulin resistance, and type 2 diabetes, while adiponectin replenishment has been shown to improve insulin resistance and impaired glucose tolerance in mice^{18–21}. Recent studies have suggested that CTRPs may also form heteromeric complexes, and that adiponectin can form heteromeric proteins with CTRP2 and CTRP9^{17,22,23}.

We previously reported cloning of AdipoR1 and AdipoR2 as receptors for adiponectin²⁴. AdipoR1 and AdipoR2 were assumed to have a seven-transmembrane (7TM) topology with an internal N-terminus and an external C-terminus, opposite to that of G-protein-coupled receptors (GPCRs)²⁴. AdipoR1 and AdipoR2 serve as physiologically the most important receptors for adiponectin and play crucial roles in the regulation of glucose and lipid metabolism, as well as in inflammation and oxidative stress, *in vivo*²⁵.

AdipoR1 may partially mediate the effects of CTRP9 on vascular endothelial cells and cardiomyocytes^{22,26}. Since AdipoR1 and AdipoR2 belong to the 11-member PAQR family of transmembrane proteins²⁷, it is speculated that other PAQR family members may constitute CTRP receptors²⁶.

We have recently succeeded in determining the crystal structures of human AdipoR1 and AdipoR2, which revealed their novel structural and functional properties to the best of our knowledge, including their 7TM architecture and zinc-binding site, which were found to be clearly distinct from those of the GPCRs²⁸. Of note, Vailiaukaitė-Brooks et al. recently provided insight into the AdipoR1 and AdipoR2 structures and reported that AdipoRs exhibit ceramidase activity, while extremely low, concluding that further studies are required to fully characterize the enzymatic parameters and substrate specificity of AdipoRs²⁹. In this regard, adiponectin administration has previously been reported to decrease ceramide levels in the liver and other tissues, and AdipoR-mediated ceramidase activity has been suggested to increase insulin sensitivity³⁰. However, given that their catalytic activity is relatively low compared to other enzymes even after stimulation with adiponectin^{29,31}. Therefore, it is suggested that AdipoR1 and/or AdipoR2 act on ceramides as any hydrolase and actually possess another lipid hydrolytic activity³¹. In addition, Scherer et al. described the possibility that AdipoRs possess another lipid hydrolase activity that could govern downstream signal transduction³². Thus, additional studies are required to define the enzymatic characteristics of these therapeutically important AdipoRs³¹. Moreover, the crystal structure of human alkaline ceramidase type 3 (ACER3) reported in 2018 was shown to possess seven alpha-helices forming a 7-transmembranes architecture with opposite N- and C-terminus domains, as with like AdipoRs³³. While, the overall architecture of ACER3 was shown to be similar to the AdipoRs, however, significant/major differences were observed between ACER3 and AdipoRs³³. These differences may have some impact on their intrinsic enzymatic properties of ACER3 versus AdipoRs, i.e. K_M parameters and substrate preference³³.

AdipoR1 and AdipoR2 serve as major receptors for adiponectin *in vivo*, where AdipoR1 and AdipoR2 are shown to activate the AMPK³⁴ and PPAR α ³⁵ pathways, respectively^{24,36,37}. AdipoR expression is shown to be decreased in obesity³⁸, where analysis of systemic glucose and lipid metabolism in systemic AdipoR1-R2 double-knockout (DKO) mice demonstrated that the AdipoRs play a critical role in glucose and lipid metabolism^{25,39}.

Then, analysis of muscle-specific AdipoR1-knockout mice showed that AdipoR1 in muscle is implicated in the regulation of mitochondrial function via Ca^{2+} signaling and the AMPK/SIRT1 pathways as well as insulin sensitivity and exercise endurance⁴⁰. However, it remains to be determined whether upregulation of AdipoR1 in muscle to a physiological level is sufficient to ameliorate insulin resistance and impaired exercise endurance in obese diabetic mice.

Identifying ways to activate adiponectin/AdipoR signaling is expected to pave the way for the development of definitive therapies for the metabolic syndrome, type 2 diabetes, and atherosclerosis. In this connection, we have succeeded in identifying an orally active synthetic small-molecule AdipoR agonist, AdipoRon by screening a library of candidate compounds³⁹. AdipoRon has been shown to exert anti-diabetic effects via mouse AdipoR, since AdipoRon failed to show any effect in DKO mice. Moreover, AdipoRon could prolong shortened lifespan observed in obese diabetic mice^{39,41,42}. It is of extreme importance to clarify if AdipoRon may represent an anti-diabetic agent in humans as a step toward developing therapeutics for lifestyle-related diseases associated with obesity. However, it still remains unclear whether AdipoRon could actually activate the human AdipoRs, and at the same time exert anti-diabetic effects *in vivo*.

In this study, by genetically engineering muscle-specific human AdipoR1-transgenic (Tg) mice, we investigated whether augmentation of AdipoR1 expression in the muscle may have a similar role to exercise in muscle mitochondria synthesis and whether AdipoR1 signaling may be associated with anti-diabetic effects. We further engineered AdipoR1-humanized mice by cross-breeding muscle-specific human AdipoR1-Tg mice and DKO mice and investigated whether or not the small-molecule AdipoR agonist may act on human AdipoR1 thus exerting anti-diabetic effects.

Results

Increased muscle insulin sensitivity and exercise endurance in muscle-human AdipoR1-Tg mice. In order to perform gain-of-function experiments to elucidate the physiological and pathophysiological roles of increased expression of human AdipoR1 in skeletal muscle in the regulation of metabolism on a long-term basis *in vivo*, we generated muscle-specific human AdipoR1-Tg (muscle-human R1-Tg) mice (Supplementary Fig. 1a). Several transgenic lines on a C57BL6 background (B6) were obtained. We quantitatively measured human ADIPOR1 and mouse AdipoR1 gene expression in skeletal muscle of muscle-human R1-Tg mice by real-time PCR analysis using a plasmid containing human and/or mouse AdipoR1 as a control. Real-time PCR analysis identified human ADIPOR1 mRNA to the ratio of approximately 0.7–1.3 folds (line 111 and line 241, respectively) of endogenous mouse mRNA in skeletal muscle (Supplementary Fig. 1b). Moreover, we determined the protein levels of human and mouse AdipoR1-R2 by western blots (Supplementary Fig. 1c, d), and found that the trends in protein levels of AdipoR1 were consistent with those in mRNA levels (Supplementary Fig. 1b). Furthermore, by western blots we confirmed abrogation of AdipoR1 and AdipoR2 proteins in AdipoR1-R2 DKO and expression of AdipoR1 protein, but not that of AdipoR2 protein, in AdipoR1-humanized mice (Supplementary Fig. 1d). We confirmed that both mice lines showed similar phenotypes in glucose tolerance

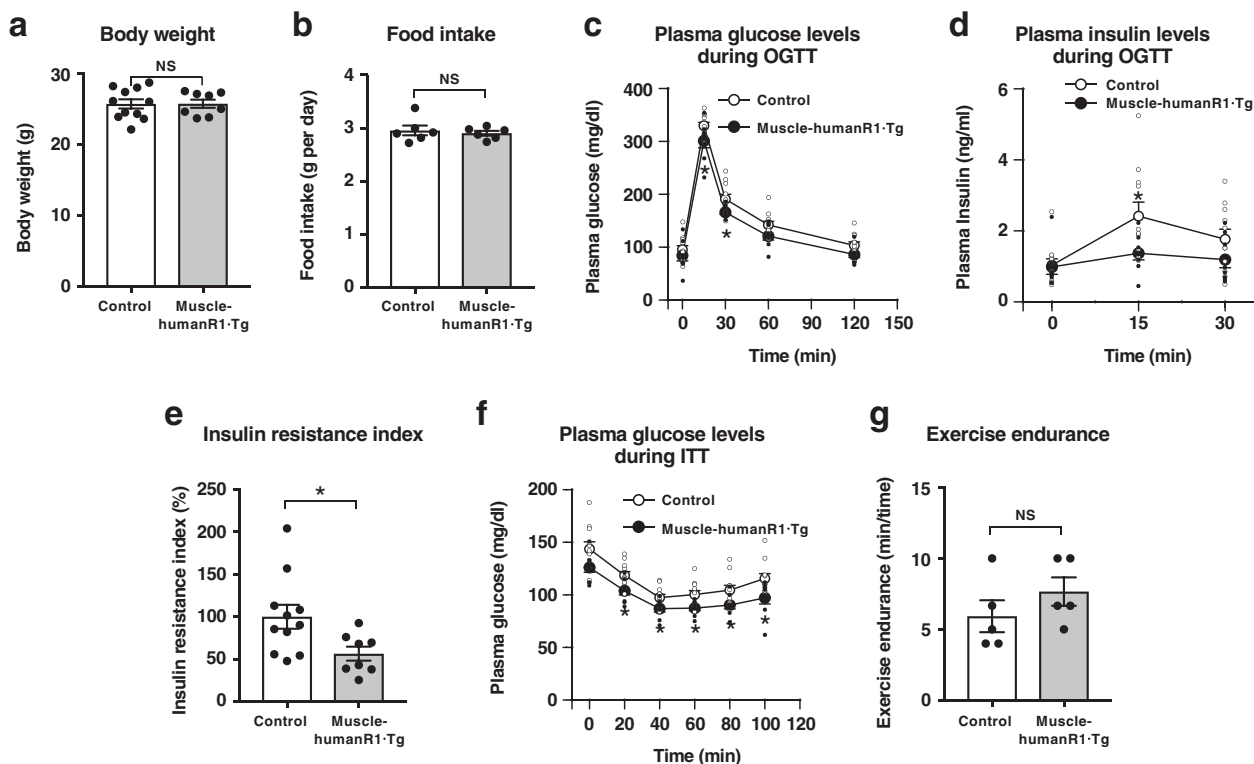


Fig. 1 Muscle-specific upregulation of human AdipoR1 increases insulin sensitivity on a normal chow diet. Body weight (a), food intake (b), plasma glucose (c), plasma insulin (d) and insulin resistance index (e) during oral glucose tolerance test (OGTT) (1.5 g glucose per kg body weight), plasma glucose (f) during insulin tolerance test (ITT) (0.25 U insulin per kg body weight) and exercise endurance (g). All values are presented as means \pm s.e.m. * $P < 0.05$ and ** $P < 0.01$ compared to control mice (unpaired two-tailed t-test). NS, not significant. Control mice: $n = 11$; muscle-humanR1-Tg mice: $n = 8$ (a, c, d, e, f) $n = 6$ each (b), $n = 5$ each (g).

and insulin resistance on both on the normal chow and high-fat diet (Figs. 1, 2, Supplementary Figs. 2, 3). Therefore, we carried out further experiments using line 241. Expression of human AdipoR1 within the physiological range in skeletal muscle did not significantly affect body weight (Fig. 1a) nor food intake (Fig. 1b) in mice on a normal chow diet, but it did significantly reduce plasma glucose levels at 15 and 30 min, tended to reduce plasma glucose levels at 60 and 120 min, and also significantly reduced plasma insulin levels at 15 min after oral glucose administration (Fig. 1c, d). Muscle-human R1-Tg mice fed a normal chow had a significantly reduced insulin resistance index (Fig. 1e). Moreover, muscle-human R1-Tg mice fed a normal chow diet tended to exhibit lower plasma glucose levels, and exhibited significantly lower plasma glucose levels than control mice during insulin tolerance tests (Fig. 1f). Furthermore, muscle-human R1-Tg mice fed a normal chow diet tended to exhibit increased exercise endurance (Fig. 1g).

We next tried to clarify the beneficial effects of upregulation of AdipoR1 in skeletal muscle in high-fat-diet-induced obese mice. Expression of human AdipoR1 in skeletal muscle did not significantly affect body weight (Fig. 2a) nor food intake (Fig. 2b) in mice on a high-fat diet, but it did significantly reduce fasting plasma triglyceride levels (Fig. 2c), plasma glucose and insulin levels before and during oral glucose tolerance tests (OGTTs) (Fig. 2d, e). The decrease in glucose levels in the face of reduced plasma insulin levels indicates improved insulin sensitivity, and the expression of human AdipoR1 in skeletal muscle indeed reduced insulin resistance index in mice on a high-fat diet (Fig. 2f). The glucose-lowering effect of exogenous insulin was also greater in muscle-human R1-Tg mice than in control mice fed a high-fat diet (Fig. 2g).

To study the impact of human AdipoR1 expression on skeletal muscle function in intact animals, we challenged control and muscle-human R1-Tg mice with involuntary physical exercise assessed by treadmill running. Importantly, muscle-human R1-Tg mice fed a high-fat diet exhibited significantly increased exercise endurance (Fig. 2h).

We next performed hyperinsulinaemic euglycaemic clamp experiment in mice on a high-fat diet. The glucose infusion rate was significantly increased (Fig. 2i), the endogenous glucose production was not altered (Fig. 2j), and the glucose disposal rate was significantly increased (Fig. 2k) in muscle-human R1-Tg mice fed a high-fat diet, indicating increased insulin sensitivity in muscle.

In agreement with the data obtained from the hyperinsulinaemic euglycaemic clamps, insulin-stimulated phosphorylation of Ser 473 in Akt was increased in skeletal muscle of muscle-human R1-Tg mice fed a high-fat diet (Fig. 2l).

Increased PGC-1 and mitochondrial genes in muscle-human AdipoR1-Tg. To clarify the molecular mechanisms by which muscle-specific upregulation of AdipoR1 increases insulin sensitivity and exercise endurance, we performed gene expression analyses. High-fat diet significantly decreased the expression of genes involved in mitochondrial biogenesis such as *Ppargc1a*⁴³ (Fig. 3a) and estrogen-related receptor α (*Esrra*)⁴⁴ (Fig. 3b), transcription such as nuclear respiratory factor 1 (*Nrf1*) (Fig. 3c), mitochondrial DNA replication/translation such as mitochondrial transcription factor A (*Tfam*) (Fig. 3d), oxidative phosphorylation such as cytochrome c oxidase subunit II (*mt-Co2*) (Fig. 3e), and mitochondrial oxidative stress-detoxification such as manganese superoxide dismutase (*Sod2*) (Fig. 3f).

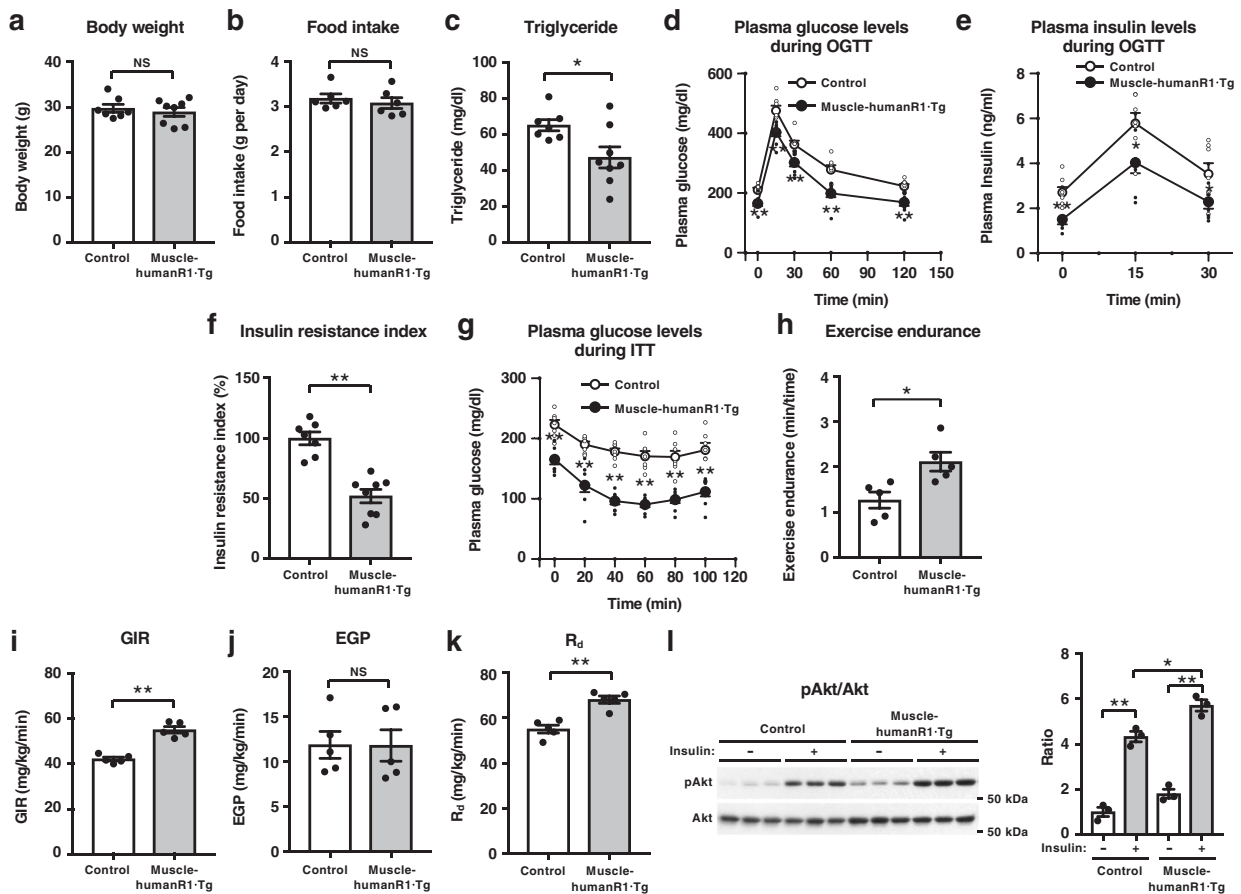


Fig. 2 Muscle-specific upregulation of human AdipoR1 increases insulin sensitivity and exercise endurance on a high-fat diet. Body weight (**a**), food intake (**b**), plasma triglyceride (**c**), plasma glucose (**d**), plasma insulin (**e**), and insulin resistance index (**f**) during oral glucose tolerance test (OGTT) (1.0 g glucose per kg body weight), plasma glucose (**g**) during insulin tolerance test (ITT) (0.5 U insulin per kg body weight), exercise endurance (**h**), glucose infusion rate (GIR) (**i**), endogenous glucose production (EGP) (**j**) and rates of glucose disposal (R_d) (**k**) during hyperinsulinemic euglycemic clamp study in control and muscle-humanR1-Tg mice on a high-fat diet. Phosphorylation and amount of Akt (**l**) in skeletal muscle treated with or without insulin (0.3 U per kg body weight) for 7.5 min in control and muscle-humanR1-Tg mice on a high-fat diet. All values are presented as means \pm s.e.m. * $P < 0.05$ and ** $P < 0.01$ compared to control mice (unpaired two-tailed t-test). NS, not significant. Control mice: $n = 7$; muscle-humanR1-Tg mice: $n = 8$ (**a**, **c**, **d**, **e**, **f**, **g**), $n = 6$ each (**b**), $n = 5$ each (**h**, **i**, **j**, **k**), $n = 3$ each (**l**).

Importantly, expression of human AdipoR1 in skeletal muscle of mice fed a high-fat diet significantly increased the expression of genes involved in mitochondrial biogenesis such as *Ppargc1a* (Fig. 3a) and *Esrra* (Fig. 3b), transcription such as *Nrf1* (Fig. 3c), mitochondrial DNA replication/translation such as *Tfam* (Fig. 3d), oxidative phosphorylation such as *mt-Co2* (Fig. 3e), and mitochondrial oxidative stress-detoxification such as *Sod2* (Fig. 3f).

We next examined the expression of metabolic genes and found that genes involved in fatty-acid oxidation, such as medium-chain acyl-CoA dehydrogenase (*Acadm*)⁴⁵, were significantly increased in muscle-human R1-Tg mice fed a high-fat diet (Fig. 3g), which is consistent with significantly decreased plasma triglyceride levels (Fig. 2c).

The expression of human AdipoR1 in skeletal muscle of mice fed a high-fat diet increased the levels of the oxidative, high endurance type I fiber⁴⁶ marker troponin I (slow) (*Tnni1*) (Fig. 3h), which was consistent with increased exercise endurance in muscle-human R1-Tg mice fed a high-fat diet (Fig. 2h). High-fat diet significantly decreased expression of the insulin-sensitive glucose transporter 4 (*Slc2a4*), while expression of human AdipoR1 in skeletal muscle of mice fed a high-fat diet increased its expression (Fig. 3i).

We next attempted to examine whether exercise could reverse the alterations of genes expression observed in high-fat-diet-induced obese diabetic mice. We challenged mice with involuntary physical exercise by treadmill running. The treadmill exercise regimen was 15 m min⁻¹ for 30 min. Two weeks' exercise significantly increased genes involved in mitochondrial biogenesis such as *Ppargc1a* (Fig. 3a) and *Esrra* (Fig. 3b), transcription such as *Nrf1* (Fig. 3c), mitochondrial DNA replication/translation such as *Tfam* (Fig. 3d), oxidative phosphorylation such as *mt-Co2* (Fig. 3e), mitochondrial oxidative stress-detoxification such as *Sod2* (Fig. 3f) as well as oxidative, high endurance type I fiber marker *Tnni1* (Fig. 3h) and *Slc2a4* (Fig. 3i) to almost the same extents as the expression of human AdipoR1 in skeletal muscle. These data revealed that the expression of human AdipoR1 and exercise-induced alterations in the expression of these genes in skeletal muscle to very similar extents, and that upregulation of AdipoR1 in skeletal muscle could be exercise-mimetics. These findings were consistent with those of the histological analysis also performed (Fig. 3j). In soleus muscle of muscle-human R1-Tg mice fed a high-fat diet, type I fibers were increased by 15% (Fig. 3j). Two weeks' exercise significantly increased type I fibers in the soleus muscle of mice fed a high-fat diet (Fig. 3j).

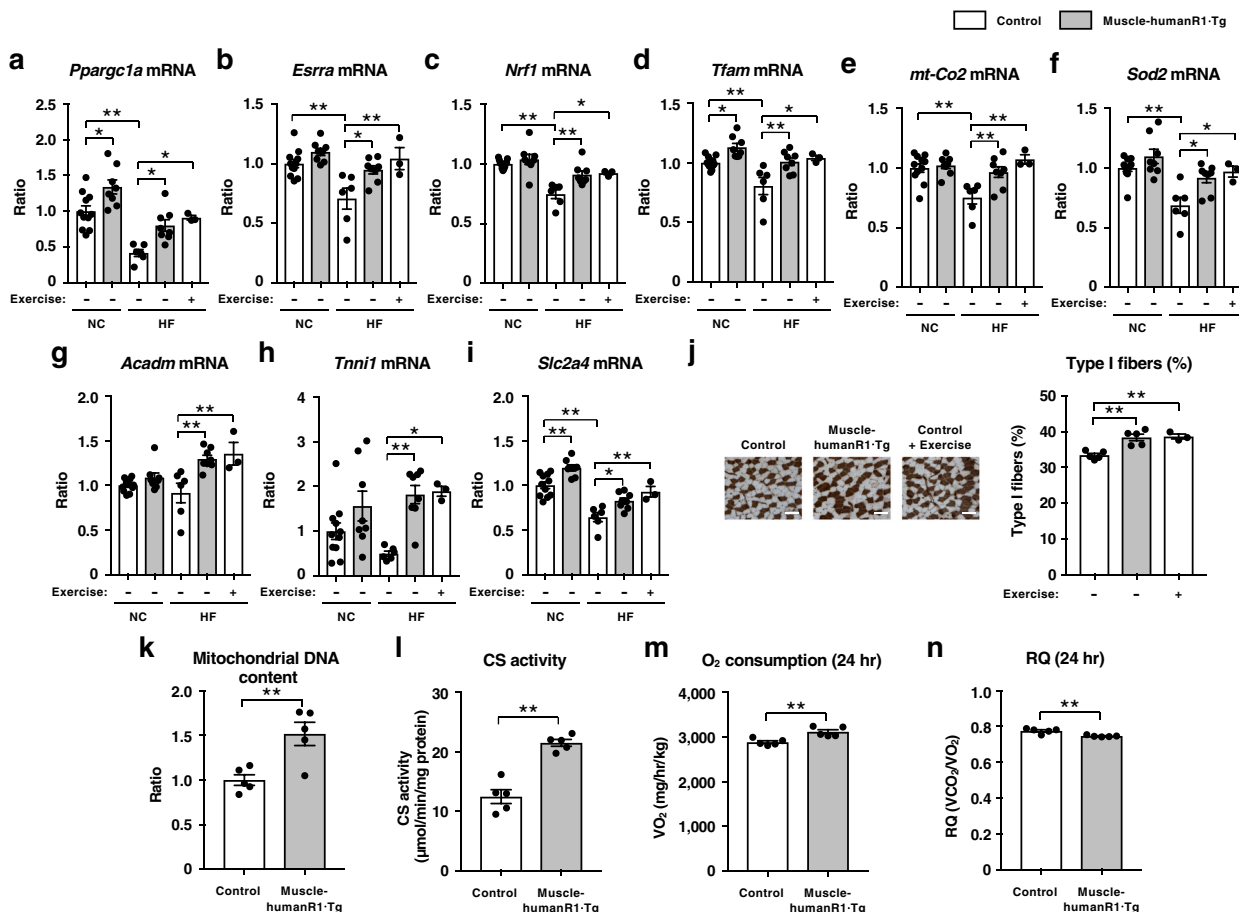


Fig. 3 Muscle-specific upregulation of human AdipoR1 increases genes involved in mitochondrial biogenesis and oxidative stress-detoxification on a normal chow or a high-fat diet. *Pparg1a* (a), *Esrra* (b), *Nr1f1* (c), *Tfam* (d), *mt-Co2* (e), *Sod2* (f), *Acadm* (g), *Tnni1* (h) and *Slc2a4* (i) mRNA levels in skeletal muscle from control and muscle-humanR1-Tg mice on a normal chow (NC) or a high-fat (HF) diet. Control mice on a NC diet ($n = 11$); muscle-humanR1-Tg mice on a NC diet ($n = 8$). Control mice on a HF diet ($n = 6$); muscle-humanR1-Tg mice on a HF diet ($n = 8$); control mice on a HF diet after 2 weeks exercise ($n = 3$). ATPase (pH 4.3 for type I fibers) staining of soleus muscle (j) (scale bars, 100 μ m), quantification of type I fibers based on fiber-type analyses in soleus muscle from control and muscle-humanR1-Tg mice on a HF diet and control mice on a HF diet after 2 weeks exercise. Control mice on a HF diet ($n = 5$); muscle-humanR1-Tg mice on a HF diet ($n = 5$); control mice on a HF diet after 2 weeks exercise ($n = 3$). Mitochondrial DNA content (k) as assessed by mitochondrial DNA copy number and citrate synthase (CS) enzyme activity (l) in skeletal muscle from control and muscle-humanR1-Tg mice on a HF diet. Control mice on a HF diet ($n = 5$); muscle-humanR1-Tg mice on a HF diet ($n = 5$). Oxygen (O₂) consumption (m) and respiratory quotient (RQ) (n) in control and muscle-humanR1-Tg mice on a HF diet. $n = 5$ each. All values are presented as means \pm s.e.m. * $P < 0.05$ and ** $P < 0.01$ compared to control mice or as indicated. P values were determined ANOVA followed by Tukey-Kramer multiple comparison tests (a-j) or unpaired two-tailed t-test (k-n). NS, not significant.

Moreover, muscle-human R1-Tg mice fed a high-fat diet had an increased mitochondrial DNA content (Fig. 3k) and citrate synthase activity (Fig. 3l) in skeletal muscle. Furthermore, analysis of the mitochondrial morphology by electron microscopy revealed that exercise training increases skeletal muscle mitochondrial volume density by enlarging existing mitochondria⁴⁷. The mitochondria of skeletal muscle in muscle-human R1-Tg mice fed a high-fat diet appeared to be slightly enlarged compared to that of control mice, similar to exercise (Supplementary Fig. 4). These data indicated that the expression of human AdipoR1 increased mitochondria biogenesis in skeletal muscle.

Muscle-human R1-Tg mice fed a high-fat diet had significantly increased O₂ consumption (Fig. 3m) but decreased RQ (Fig. 3n). These data suggested that the expression of human AdipoR1 in skeletal muscle resulted in increases in fatty-acid oxidation.

Beneficial effects of AdipoRon via human AdipoR1 in skeletal muscle. We previously showed that orally active AdipoR agonist AdipoRon ameliorated insulin resistance and glucose intolerance

in mice fed a high-fat diet, which was completely obliterated in AdipoR1 and AdipoR2 DKO (mouse R1-R2DKO) mice³⁹. For the development of clinically available drug, it is extremely important to clarify whether AdipoRon could exert its beneficial effects via human AdipoR. To address this critically important issue, we next generated mouse R1-R2DKO mice expressing human AdipoR1 in skeletal muscle (AdipoR1-humanized mice).

We next studied the dose-dependent effects of AdipoRon in AdipoR1-humanized mice fed a high-fat diet. Orally administered AdipoRon reduced plasma glucose levels in a dose-dependent manner (Supplementary Fig. 5a). Furthermore, when orally administered at higher doses, AdipoRon (100–250 mg per kg body weight) did not cause hypoglycaemia, and observed no abnormality and no signs of toxicity (Supplementary Fig. 5b).

As we previously showed, oral administration of AdipoRon (50 mg per kg body weight) for 10 days had no effects on body weight (Fig. 4a) nor food intake (Fig. 4b), and could not ameliorate hyperglycemia (Fig. 4c) nor hyperinsulinemia (Fig. 4d) in mouse R1-R2DKO mice fed a high-fat diet. AdipoRon also had no effects

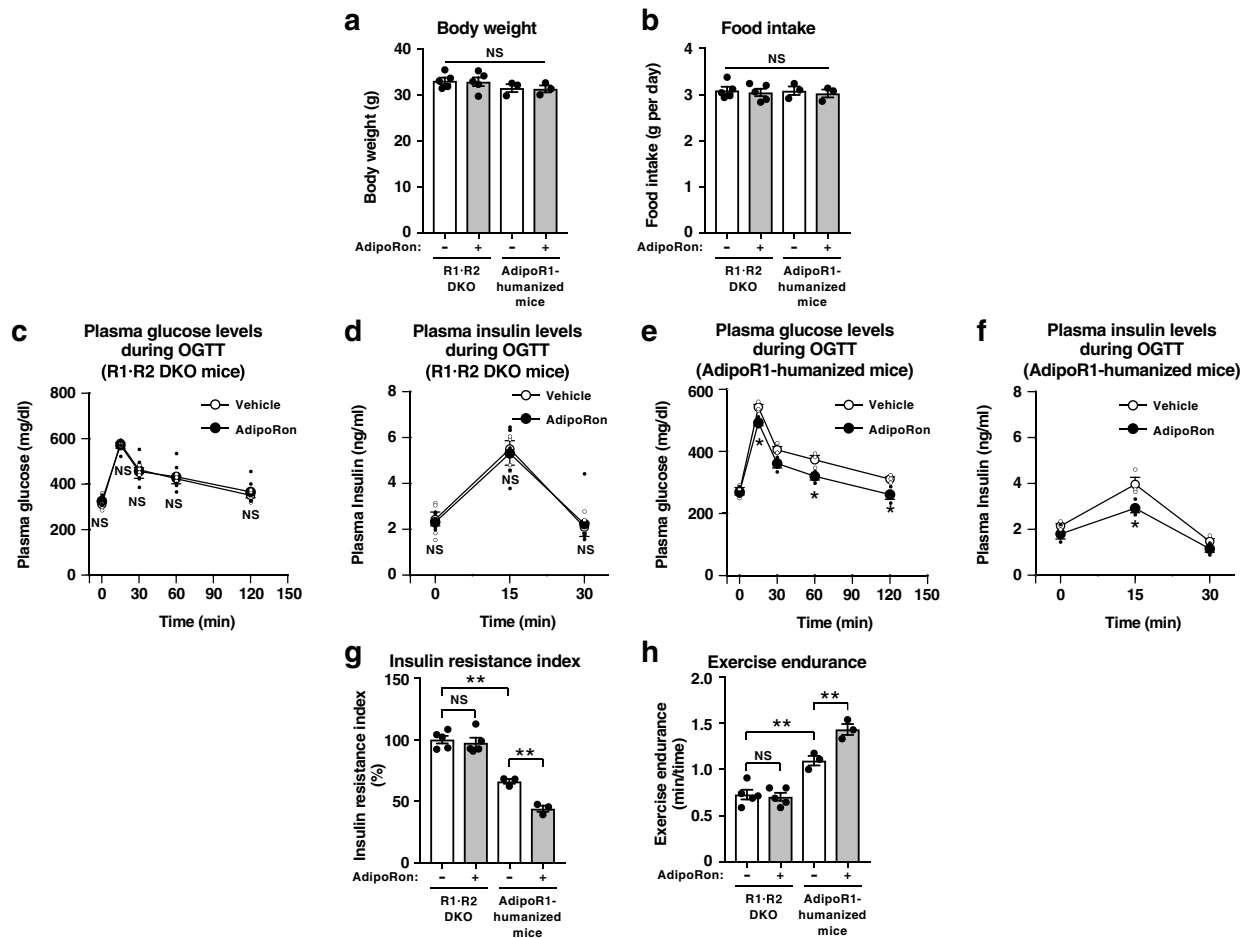


Fig. 4 AdipoRon could increase insulin sensitivity and exercise endurance in AdipoR-humanized mice on a high-fat diet. Body weight (**a**), food intake (**b**), plasma glucose (**c**, **e**), plasma insulin (**d**, **f**) and insulin resistance index (**g**) during oral glucose tolerance test (OGTT) (1.0 g glucose per kg body weight), exercise endurance (**h**) in mouse R1-R2DKO mice and muscle-humanR1-Tg/mouse R1-R2DKO (AdipoR1-humanized) mice on a high-fat diet, treated once daily oral administration of AdipoRon (50 mg per kg body weight) for two weeks. All values are presented as means \pm s.e.m. * $P < 0.05$ and ** $P < 0.01$ compared to control mice or as indicated. P values were determined ANOVA followed by Tukey-Kramer multiple comparison tests (**a**, **b**, **g**, **h**) or unpaired two-tailed t-test (**c**-**f**). NS, not significant. R1-R2DKO mice (Vehicle: $n = 5$; AdipoRon: $n = 5$), muscle-AdipoR1-humanized mice (Vehicle: $n = 3$; AdipoRon: $n = 3$).

on body weight (Fig. 4a) nor food intake (Fig. 4b) in AdipoR1-humanized mice fed a high-fat diet, importantly, AdipoRon could significantly decrease plasma glucose levels (Fig. 4e) and plasma insulin levels (Fig. 4f) during OGTT and also insulin resistance index (Fig. 4g), indicating that AdipoRon could indeed ameliorate insulin resistance and glucose intolerance via human AdipoR1 in skeletal muscle. The expression of human AdipoR1 in skeletal muscle in mouse R1-R2DKO mice ameliorated insulin resistance and increased exercise endurance (Fig. 4g, h).

We challenged mice fed a high-fat diet with involuntary physical exercise by treadmill running and then assessed muscle endurance. AdipoRon significantly increased exercise endurance in AdipoR1-humanized mice, but not in R1-R2DKO mice fed a high-fat diet (Fig. 4h). These data clearly indicated that AdipoRon could increase exercise endurance via human AdipoR1 in the skeletal muscle of mice fed a high-fat diet.

Intravenous injection of AdipoRon (50 mg per kg body weight) significantly induced phosphorylation of AMPK in skeletal muscle of AdipoR1-humanized mice, but not in R1-R2DKO mice (Fig. 5a) fed a high-fat diet. These data clearly indicated that AdipoRon could activate AMPK in skeletal muscle via human AdipoR1 in skeletal muscle of mice fed a high-fat diet.

Orally administered AdipoRon significantly increased expression levels of genes involved in mitochondrial biogenesis such as *Ppargc1a* (Fig. 5b) and genes involved in oxidative phosphorylation such as *mt-Co2* (Fig. 5c) in skeletal muscle of AdipoR1-humanized mice, but not in R1-R2DKO mice fed a high-fat diet. Moreover, AdipoRon significantly increased expression levels of oxidative, high endurance type I fiber marker *Tnni1* (Fig. 5d) and genes involved in mitochondrial oxidative stress-detoxification such as *Sod2* (Fig. 5e) in skeletal muscle of AdipoR1-humanized mice, but not in R1-R2DKO mice fed a high-fat diet. Treatment of R1-R2DKO mice with AdipoRon failed to increase type I fibers in skeletal muscle (Fig. 5f). AdipoRon significantly increased the ratio of type I fibers in skeletal muscle of AdipoR1-humanized mice (Fig. 5f). These data clearly indicated that AdipoRon could exert its beneficial effects in skeletal muscle via human AdipoR1 in skeletal muscle of mice fed a high-fat diet.

We found that AdipoRon significantly decreased the expression of *Pck1* and *G6pc* in the liver of wild-type mice but not in that of R1-R2DKO mice fed a high-fat diet³⁹. AdipoRon increased the expression levels of the gene encoding PPAR α itself and its target genes, including those involved in fatty-acid combustion such as acyl-CoA oxidase (*Acox1*), those involved in energy

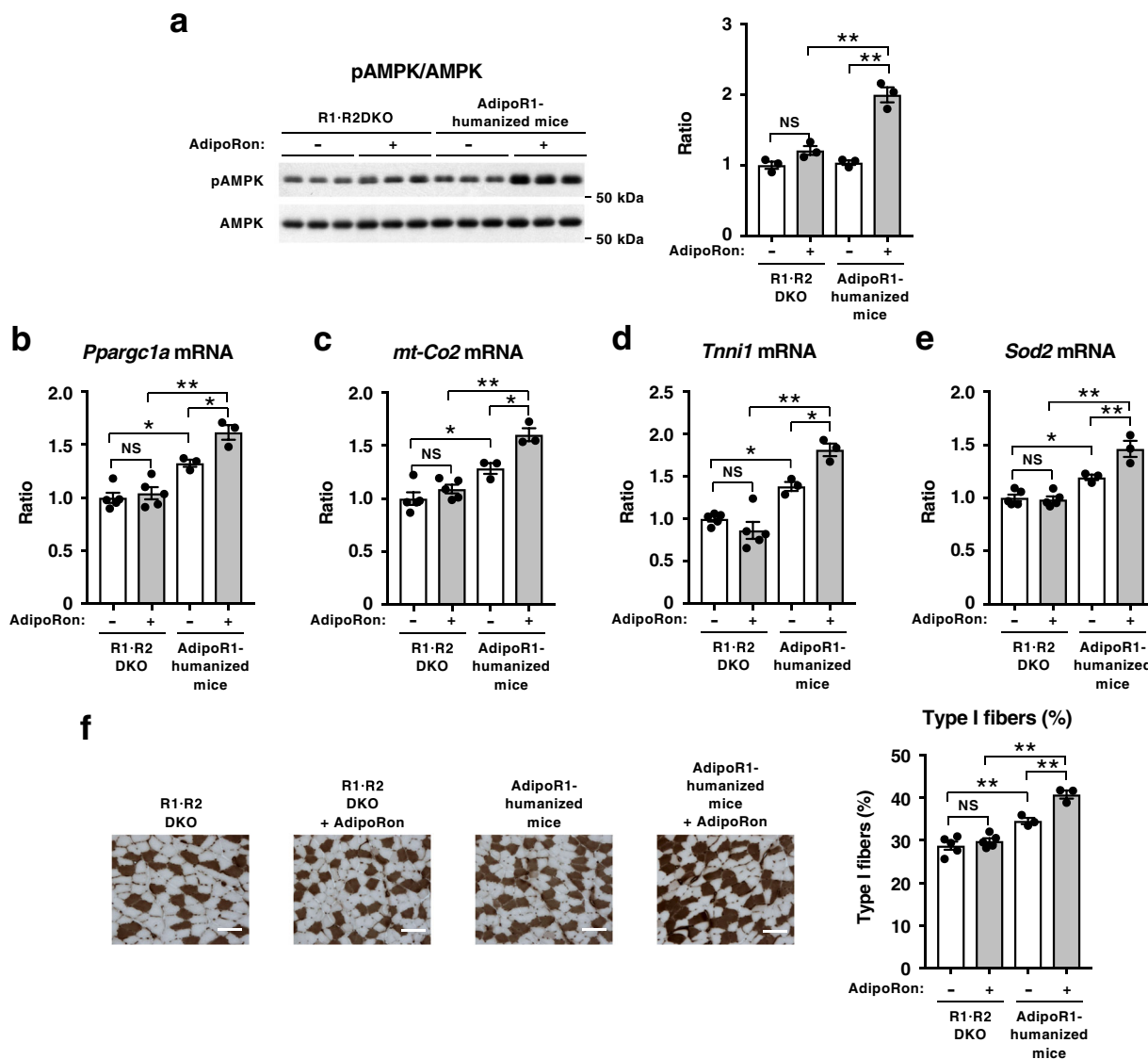


Fig. 5 AdipoRon could increase pAMPK and genes involved in mitochondrial biogenesis as well as oxidative stress-detoxification in AdipoR1-humanized mice on a high-fat diet. Phosphorylation and amount of AMPK (**a**) in skeletal muscle from R1-R2DKO mice or AdipoR1-humanized mice on a high-fat diet, treated for 7.5 min after injection of 50 mg of AdipoRon per kg body weight intravenously into mice through an inferior vena cava catheter. *Ppargc1a* (**b**), *mt-Co2* (**c**), *Tnni1* (**d**) and *Sod2* (**e**) mRNA levels in skeletal muscle from R1-R2DKO mice or AdipoR1-humanized mice on a high-fat diet, treated once daily oral administration of AdipoRon (50 mg per kg body weight) for two weeks. ATPase (pH 4.3 for type I fibers) staining of soleus muscle (**f**) (scale bars, 100 μ m), quantification of type I fibers based on fiber-type analyses in soleus muscle from R1-R2DKO mice and AdipoR1-humanized mice on a high-fat diet with or without AdipoRon (50 mg per kg body weight). All values are presented as means \pm s.e.m. * $P < 0.05$ and ** $P < 0.01$ compared to control mice or as indicated (ANOVA followed by Tukey-Kramer multiple comparison tests). NS, not significant. $n = 3$ each (**a**) R1-R2DKO mice (Vehicle: $n = 5$; AdipoRon: $n = 5$), AdipoR1-humanized mice (Vehicle, $n = 3$; AdipoRon, $n = 3$) (**b-f**).

dissipation such as uncoupling protein 2 (*Ucp2*) in the liver of wild-type mice but not in that of R1-R2DKO mice fed a high-fat diet³⁹. However, the expression of human AdipoR1 in skeletal muscle of R1-R2DKO mice caused no change in the expression of *Pck1*, *G6pc*, *Acox1*, and *Ucp2* in the liver (Supplementary Fig. 6a–d).

AdipoRon reduced the expression levels of genes encoding pro-inflammatory cytokines such as *Tnf* and *Ccl2* in the epididymal white adipose tissue (eWAT) of AdipoR1-humanized mice but not in that of R1-R2DKO mice fed a high-fat diet (Supplementary Fig. 6e, f). Moreover, AdipoRon reduced the levels of markers for classically activated M1 macrophages such as CD11c (*Itgax*), but not the levels of markers for the alternatively activated M2 macrophages such as CD206 (*Mrc1*) in the eWAT of AdipoR1-

humanized mice fed a high-fat diet, while these changes were not observed in R1-R2DKO mice (Supplementary Fig. 6g, h). In contrast to eWAT, no appreciable change was seen in expression levels of genes encoding pro-inflammatory cytokines and macrophage markers in the inguinal white adipose tissue (iWAT) of AdipoR1-humanized mice (Supplementary Fig. 6i–l). These data suggested that the expression of human AdipoR1 in skeletal muscle resulted in increases anti-inflammatory effects in eWAT.

Discussion

We engineered muscle-specific human AdipoR1-transgenic mice in this study and demonstrated that enhancing AdipoR1 expression in muscle play a role in the regulation of mitochondria-related

genes and that it also improves impaired glucose tolerance and insulin resistance in mouse models of obesity and type 2 diabetes. PGC-1 α serves as a key regulator of mitochondrial biogenesis and function in muscle^{43,48}. Of note here is the fact that the expression of AdipoR1, as well as that of PGC-1 α , has been reported to be decreased in obese, diabetic db/db mice or in type 2 diabetic patients^{40,49}. Our present experiments also showed that the expression of AdipoR1, PGC-1 α and mitochondria-related genes was decreased in mice fed a high-fat diet. Importantly, the co-expression of both human AdipoR1 and mouse endogenous AdipoR1, yielding a 2-fold upregulation of AdipoR1, was shown to result in significantly increased expression of PGC-1 α and mitochondria-related genes, as well as increased molecules involved in mitochondrial oxidative stress-detoxification. These alterations collectively resulted in improvements in impaired glucose tolerance and insulin resistance in mice fed a high-fat diet. Thus, we have demonstrated for the first time in this study that the upregulation of AdipoR1 in muscle is sufficient to ameliorate insulin resistance and impaired exercise endurance in obese diabetic mice.

Exercise has been reported to activate the Ca²⁺ signaling, AMPK, and PGC-1 α pathways, and at the same time improve glucose tolerance and insulin resistance. Thus exercise is likely to exert beneficial effects on obesity-related disease, such as type 2 diabetes, and may contribute to healthy longevity^{1,40,48,50,51}. Strikingly, our study showed that muscle-specific AdipoR1 upregulation led to the expression of mitochondria-related genes being recovered, with the extent of their recovery found to be similar to that in high-fat diet-fed mice subjected to exercise, suggesting that upregulation of AdipoR1 may represent “exercise-mimetics”.

Incidentally, of note, another group has reported that their AdipoR1-R2 DKO mice died during their development⁵² and that they were derived from AdipoR2-knockout mice exhibiting a phenotype opposite to that of adiponectin-knockout mice characterized by aggravating of insulin resistance and atherosclerosis^{53–55}. Thus, the difference between the two AdipoR1-R2 DKO mice seems to be due to differences in their knockout mice constructs. Indeed, we have demonstrated that neither AdipoR1 nor AdipoR2 is expressed in AdipoR1-R2 DKO mice (Supplementary Fig. 1d). On the other hand, Lindgren et al. used heterozygous AdipoR1 and AdipoR2 gene knockout mice obtained from Deltagen (San Carlos, CA) in their experiments⁵². Briefly, the mice were generated by gene targeting through homologous recombination in 129/OlaHsd ES cells using target vectors that contained the following cassette: lacO-splice acceptor-internal ribosomal entry site-lacZ-poly A-phosphoglycerate kinase promoter-neomycin resistance-poly A (PGK-neo)⁵². Very importantly, the other allele, which retained PGK-neo and led to additional phenotypes, demonstrating that the expression of other genes was affected^{56–58}. It was thus suggested that the AdipoR1-R2 DKO mice used by Lindgren et al.⁵² may have affected the expression of other genes besides AdipoR1-R2.

The metabolic syndrome and type 2 diabetes are counted among the major causes of cardiovascular disease and cancer as leading causes of death in humans^{59–61}, which has led to mounting expectations for radical therapeutics for obesity-related diseases, such as type 2 diabetes. Despite the wide range of therapeutics aimed at improving insulin resistance currently available, however, the number of type 2 diabetic patients continues to increase, suggesting that there still remains a considerable unmet need in anti-diabetic treatment. Against this background, small-molecule AdipoR agonists are drawing attention as a potential another class of drugs for obesity-related diseases including type 2 diabetes^{62,63}. We have demonstrated for the first time in this study that one of these compounds,

AdipoRon, acts on human AdipoR1, activates the AMPK pathway downstream, and augments the expression of mitochondria-related genes, thus improving impaired glucose tolerance and insulin resistance in vivo. These findings appear to provide proof of concept that the small-molecule AdipoR agonist may have the potential to work not only in mice but in humans, whose observation is required for its clinical development. By measuring molecular interactions using a Biacore system, AdipoRon has been shown to directly bind to human AdipoRs in vitro³⁹.

After oral administration of 50 mg per kg body weight of AdipoRon to C57BL/6 wild-type mice, we found that the half-life of AdipoRon was 2 h, and the maximal concentration (C_{max}) of AdipoRon was 11.8 μ M³⁹. The half-life of the glucose-lowering effect of AdipoRon was 8 h. After the maximum concentration was reached at 30 min, the glucose-lowering effect became maximal at 2 h, and lasted for at least 8 h and even after AdipoRon was cleared from plasma. Importantly, AdipoRon did prolong the shortened lifespan of obese diabetic mice.

Based on the information obtained from structures of AdipoRs²⁸, much progress has recently been made in the analysis of the co-crystal structure of AdipoRs and AdipoRon as well as in the development of small-molecule AdipoR agonists for clinical use. Moreover, expectations are mounting for the development of small-molecule AdipoR agonists for use as anti-diabetic agents.

Thus, the small-molecule AdipoR agonist appears to promise to become an effective therapeutic modality for lifestyle-related diseases that have obesity as a common underlying cause, promoting healthy longevity in humans.

Methods

Mouse studies. Male mice were 6–10 weeks of age at the time of the experiment. The animal care and use procedures were approved by the Animal Care Committee of the University of Tokyo. They were housed in cages and maintained on a 12 h light-dark cycle with access to chow and water ad libitum. In these experiments, we used standard chow diet with the following composition: 25.6% (wt/wt) protein, 3.8% fiber, 6.9% ash, 50.5% carbohydrates, 4% fat and 9.2% water (CE-2, CLEA Japan Inc.) or high-fat diet 32 consisting of 25.5% (wt/wt) protein, 2.9% fiber, 4.0% ash, 29.4% carbohydrates, 32% fat and 6.2% water (CLEA Japan Inc.)⁶⁴. Plasma glucose levels were determined by using a glucose B-test (Wako Pure Chemical Industries). Plasma insulin was measured with an insulin immunoassay (Shibayagi). Plasma triglyceride (Wako Pure Chemical Industries) was assayed by enzymatic methods. All measurements were performed in blinded fashion. When the mice in the same genotype received different treatments, they were randomly assigned to treatment groups.

Administration of AdipoRon. AdipoRon (Purity, 95%) was synthesized by Enamine Ltd (Kyiv, Ukraine)³⁹. For administration, AdipoRon was prepared in 0.5% hydroxypropyl methylcellulose. AdipoRon (50 mg per kg body weight) was orally administered to mice once daily for two weeks. The sampling of the mice parameters was performed 4 h after oral administration. To study AMPK phosphorylation in vivo, AdipoRon was intravenously injected at 50 mg per kg body weight into the mice through an inferior vena cava catheter. The mice were treated for 7.5 min with AdipoRon and were examined phosphorylation and amount of AMPK in skeletal muscle.

Generation of AdipoR1-humanized mice. A human AdipoR1 coding sequence cDNA²⁴ for insertion was cloned and the transgene vector CAG-LacZ-human AdipoR1, which contains a CAG gene promoter-loxP-LacZ gene-loxP-human AdipoR1 was constructed (Supplementary Fig. 1). The *ADIPOR1* transgene was microinjected into a fertilized mouse egg to produce a transgenic mouse line. Animals transgenically expressing cre recombinase under the control of the muscle creatine kinase promoter (MCK-Cre) were generous gifts from Dr. C. R. Kahn of the Joslin Diabetes Center, Boston, MA, USA⁴⁰. We backcrossed them with C57BL/6 mice more than seven times. CAG-LacZ-human AdipoR1 mice were mated with MCK-Cre mice to generate CAG-LacZ-human AdipoR1/MCK-Cre double transgenic mice. The original *Adipor1*^{+/-}/*Adipor2*^{+/-} mice (C57BL/6 and 129/Sv mixed background)²⁵ were backcrossed with C57BL/6 mice more than seven times. *Adipor1*^{-/-}/*Adipor2*^{-/-} mice were prepared by *Adipor1*^{+/-}/*Adipor2*^{+/-} mouse intercrosses²⁵. CAG-LacZ-human AdipoR1/MCK-Cre/*Adipor1*^{-/-}/*Adipor2*^{-/-} DKO mice (AdipoR1-humanized mice) were generated by crossing CAG-LacZ-human AdipoR1/MCK-Cre double transgenic mice to *Adipor1*^{-/-}/*Adipor2*^{-/-} mice. Genotyping of the mice was performed using PCR. Three primers were used for *Adipor1* genotyping: the forward primer 1 (5'-GCAGGGTAACTGATTAG

CTATG-3'), the forward primer 2 (5'-ATAGATCTCTCGTGGGATCATTG-3'), and the reverse primer (5'-TTACTGCACCTCTCTGCTGGA-3'). Three primers were used for Adipor2 genotyping: the forward primer 1 (5'-AGCCTACTGCCTACTGTATTGT-3'), the forward primer 2 (5'-ATAGATCTCTCGTGGGATCA TTG-3'), and the reverse primer (5'-ACTCTTCTAACCTTCATCAGGAG-3'). The primers for detecting rabbit beta-globin polyA were the forward primer (5'-CTGCTGTCCATTCCTATTC-3') and the reverse primer (5'-GGACAG CTATGACTGGGAGTAG-3'). The primers were used for detection of Cre were 5'-CGCCGCATAACCAGTGAAAC-3', 5'-ATGTCCAATTTACTGACCG-3'.

Insulin resistance index. The OGTT was conducted as previously described^{18,36} with slight modifications. The areas of the glucose and insulin curves were calculated by multiplying the cumulative mean height of the glucose values (1 mg ml⁻¹ = 1 cm) and insulin values (1 ng ml⁻¹ = 1 cm), respectively, by time (60 min = 1 cm)^{18,25}. The insulin resistance index was calculated from the product of the areas of glucose and insulin × 10⁻² in the glucose tolerance test. The results are expressed as the percentage of the value of control mice^{18,25}.

Hyperinsulinemic euglycemic clamp study. Clamp studies^{39,40,64,65} were carried out in mice on a high-fat diet. An infusion catheter was inserted into the right jugular vein under general anesthesia with sodium pentobarbital, 2–3 days before the study. Studies were performed on mice under conscious and unstressed conditions after a 6 h fast. A primed continuous infusion of insulin (Humulin R, Lilly) was given (10.0 milliunits kg⁻¹ min⁻¹), and the blood glucose concentration, monitored every 5 min, was maintained at 120 mg per dl by the administration of glucose (5 g of glucose per 10 ml enriched to 20% with [6,6-²H₂] glucose (Sigma)) for 120 min. Blood was sampled via tail tip bleeds at 90, 105, and 120 min for determination of the rate of glucose disappearance (Rd). Rd was calculated according to nonsteady-state equations, and endogenous glucose production (EGP) was calculated as the difference between Rd and exogenous glucose infusion rates^{39,40,64,65}.

Measurement of exercise capacity in mice. The treadmill exercise regimen was 15 m min⁻¹ for 30 min per day for 2 weeks. Exercise endurance was assessed by dividing 20 min by the number of times a mouse was unable to avoid electrical shocks.

Real-time PCR. Real-time PCR was performed according to the method described previously^{25,40}. Total RNA was prepared from cells with ISOGEN (Nippon Gene), according to the manufacturer's instructions. We used the real-time PCR method to quantify the mRNAs²⁴, with slight modifications. The real-time PCR was performed using specific TaqMan Gene Expression Assays (Applied Biosystems) for *Adipor1* (Mm01291334_mH), *Ppargc1a* (Mm00447183_m1), *Esrra* (Mm00433143_m1), *Nrfl* (Mm00447996_m1), *Tfam* (Mm00447485_m1), *mt-Co2* (Mm03294838_g1), *Sod2* (Mm00449726_m1), *Acadm* (Mm00431611_m1), *Tnmi1* (Mm00502426_m1), *Slc2a4* (Mm00436615_m1), *Pck1* (Mm00440636_m1), *G6pc* (Mm00839363_m1), *Acox1* (Mm00443579_m1), *Ucp2* (Mm00495907_g1), *Tnf* (Mm00443258_m1), *Ccl2* (Mm00441242_m1), *Itgax* (Mm01271275_m1), *Mrc1* (Mm01329361_m1) and ADIPOR1 (forward-Primer: 5'-TCCTAAGCACCGGCAGACA-3', reverse-Primer: 5'-GGCACGACGCCACTCAAG-3', Probe: 5'-AGCAGGCGTGTTC-3')

Western blot analysis. To determine insulin-stimulated phosphorylation of Ser 473 in Akt in skeletal muscle, we injected 0.3 U of insulin per kg body weight intravenously into mice through an inferior vena cava catheter. A western blot analyses were performed with anti-phosphorylated-Akt (Ser 473) (Cell Signaling Technology, 1:1000; #4060) and anti-Akt (Cell Signaling Technology, 1:1000; #9272) antibodies. To study AMPK phosphorylation in vivo, we injected 50 mg of AdipoRon per kg body weight intravenously into mice through an inferior vena cava catheter^{36,39}. Phosphorylation and protein levels of αAMPK^{66–69} were determined. Western blot analyses were performed with anti-phosphorylated-AMPK (Cell Signaling Technology #2535) and anti-αAMPK (Cell Signaling Technology, 1:1000; #2532) antibodies. To determine protein levels of AdipoR1 and AdipoR2, western blot analyses were performed with anti-AdipoR1 antibody (IBL, 1:1000; #18993), anti-AdipoR2 antibody (IBL, 1:1000; #18995), and anti-α-Tubulin (Cell Signaling Technology, 1:1000; #2125). Uncropped images of western blotting are shown in Supplementary Fig. 7.

Mitochondrial content assay. Mitochondrial content assays^{40,70} were carried out. For quantification of mitochondrial content, mtDNA in skeletal muscle was determined by qPCR⁷¹.

Citrate synthase activity. Citrate synthase activity was determined spectrophotometrically from the homogenates by using previously described methods^{47,70,72}. Briefly, measurements of citrate synthase activity were carried out at room temperature in 0.1 ml of assay medium containing 10 μg of muscle homogenate in the presence of saturating concentrations of 0.3 mM acetyl-coenzyme A, 0.1 mM dithionitrobenzoic acid and 0.5 mM oxaloacetate. The reaction was initiated by adding 0.5 mM oxaloacetate and monitored by measuring

the increase in absorbance at 412 nm due to thionitrobenzoic acid formation. All activities were normalized to mg of total protein.

Histological analyses. Histological analyses were performed according to the method described previously⁴⁰. We examined the relationship between the change in type I fiber gene expression and actual muscle fiber morphology in the skeletal muscle (soleus) of muscle-humanR1.Tg mice by using light microscopy and histochemical analysis. Samples of the muscle were frozen in liquid nitrogen-cooled isopentane. Type I and type II fibers were differentiated with myosin ATPase staining at different pH values. Specifically, at pH 4.3, type I fibers were well stained while type II fibers were not⁴⁶.

Oxygen consumption. Oxygen consumption was measured with an O₂/CO₂ metabolism measurement system for 24 h in the animals under ad libitum feeding conditions (Model MK-5000RQ; Muromachikikai, Tokyo, Japan). Each mouse was placed in a sealed chamber (560 ml volume) with an air flow of 0.65 l min⁻¹ for 24 h at room temperature. The oxygen consumed was converted to milliliters per minute by multiplying it by the flow rate.

Analyses of mitochondrial morphology by the electron microscopy. The samples were fixed with 2% paraformaldehyde and 2% glutaraldehyde in 0.1 M phosphate buffer (PB), pH 7.4 at 4 °C overnight. After this fixation the samples were washed 3 times with 0.1 M PB for 30 min each, and were postfixed with 2% osmium tetroxide in 0.1 M PB at 4 °C for 2 h. The samples were then dehydrated in graded ethanol solutions (50, 70, 90, 100%). The schedule was as follows: 50% and 70% for 30 min each at 4 °C, 90% for 30 min at room temperature, and 4 changes of 100% for 30 min each at room temperature. The samples were infiltrated with propylene oxide (PO) 2 times for 30 min each and were put into a 70:30 mixture of PO and resin (Quetol-812; Nisshin EM Co., Tokyo, Japan) for 1 h, then with the cap tubes left open, PO was volatilized overnight. The samples were transferred to a fresh 100% resin, and were polymerized at 60 °C for 48 h. The polymerized resins were ultra-thin sectioned at 70 nm with a diamond knife using an ultramicrotome (Ultracut UCT; Leica, Vienna, Austria) and the sections were mounted on copper grids. They were stained with 2% uranyl acetate at room temperature for 15 min, and then were washed with distilled water and secondary-stained with Lead stain solution (Sigma-Aldrich Co., Tokyo, Japan) at room temperature for 3 min. The grids were observed by a transmission electron microscope (JEM-1400Plus; JEOL Ltd., Tokyo, Japan) at an acceleration voltage of 100 kV. Digital images (3296 × 2472 pixels) were taken with a CCD camera (EM-14830RUBY2; JEOL Ltd., Tokyo, Japan).

Statistics and reproducibility. Results are expressed as mean ± s.e.m. Differences between two groups were assessed using unpaired two-tailed t-tests. Data involving more than two groups were assessed by analysis of variance (ANOVA) followed by Tukey-Kramer multiple comparison tests. Representative data from one of 2–5 independent experiments are shown. Every experiment was performed multiple times with essentially the same results.

Reporting summary. Further information on research design is available in the Nature Research Reporting Summary linked to this article.

Data availability

The source data for the figures are available in Supplementary Data 1. Full blots are shown in Supplementary Information. All other data that support the findings of this study are available from the corresponding author on reasonable request.

Received: 27 April 2019; Accepted: 9 December 2020;

Published online: 08 January 2021

References

- Hawley, J. A., Hargreaves, M., Joyner, M. J. & Zierath, J. R. Integrative biology of exercise. *Cell* **159**, 738–749 (2014).
- Ng, M. et al. Global, regional, and national prevalence of overweight and obesity in children and adults during 1980–2013: a systematic analysis for the Global Burden of Disease Study 2013. *Lancet* **384**, 766–781 (2014).
- Friedman, J. M. Obesity in the new millennium. *Nature* **404**, 632–634 (2000).
- Gesta, S., Tseng, Y. H. & Kahn, C. R. Developmental origin of fat: tracking obesity to its source. *Cell* **131**, 242–256 (2007).
- Glass, C. K. & Olefsky, J. M. Inflammation and lipid signaling in the etiology of insulin resistance. *Cell Metab.* **15**, 635–645 (2012).
- Lin, H. V. & Accili, D. Hormonal regulation of hepatic glucose production in health and disease. *Cell Metab.* **14**, 9–19 (2011).

7. Arita, Y. et al. Paradoxical decrease of an adipose-specific protein, adiponectin, in obesity. *Biochem. Biophys. Res. Commun.* **257**, 79–83 (1999).
8. Li, S., Shin, H. J., Ding, E. L. & van Dam, R. M. Adiponectin levels and risk of type 2 diabetes: a systematic review and meta-analysis. *JAMA* **302**, 179–188 (2009).
9. Pischon, T. et al. Plasma adiponectin levels and risk of myocardial infarction in men. *JAMA* **291**, 1730–1737 (2004).
10. Scherer, P. E., Williams, S., Fogliano, M., Baldini, G. & Lodish, H. F. A novel serum protein similar to Clq, produced exclusively in adipocytes. *J. Biol. Chem.* **270**, 26746–26749 (1995).
11. Hu, E., Liang, P. & Spiegelman, B. M. AdipoQ is a novel adipose-specific gene dysregulated in obesity. *J. Biol. Chem.* **271**, 10697–10703 (1996).
12. Maeda, K. et al. cDNA cloning and expression of a novel adipose specific collagen-like factor, apM1 (AdiPose Most abundant Gene transcript 1). *Biochem. Biophys. Res. Commun.* **221**, 286–289 (1996).
13. Nakano, Y., Tobe, T., Choi-Miura, N. H., Mazda, T. & Tomita, M. Isolation and characterization of GBP28, a novel gelatin-binding protein purified from human plasma. *J. Biochem.* **120**, 803–812 (1996).
14. Zhang, Y. et al. Positional cloning of the mouse obese gene and its human homologue. *Nature* **372**, 425–432 (1994).
15. Kahn, C. R. Triglycerides and toggling the tummy. *Nat. Genet.* **25**, 6–7 (2000).
16. Spiegelman, B. M. & Flier, J. S. Obesity and the regulation of energy balance. *Cell* **104**, 531–543 (2001).
17. Schaffler, A. & Buechler, C. CTRP family: linking immunity to metabolism. *Trends Endocrinol. Metab.* **23**, 194–204 (2012).
18. Yamauchi, T. et al. The fat-derived hormone adiponectin reverses insulin resistance associated with both lipotrophy and obesity. *Nat. Med.* **7**, 941–946 (2001).
19. Fruebis, J. et al. Proteolytic cleavage product of 30-kDa adipocyte complement-related protein increases fatty acid oxidation in muscle and causes weight loss in mice. *Proc. Natl Acad. Sci. USA* **98**, 2005–2010 (2001).
20. Berg, A. H., Combs, T. P., Du, X., Brownlee, M. & Scherer, P. E. The adipocyte-secreted protein Acrp30 enhances hepatic insulin action. *Nat. Med.* **7**, 947–953 (2001).
21. Combs, T. P., Berg, A. H., Obici, S., Scherer, P. E. & Rossetti, L. Endogenous glucose production is inhibited by the adipose-derived protein Acrp30. *J. Clin. Invest.* **108**, 1875–1881 (2001).
22. Zheng, Q. et al. Clq/TNF-related proteins, a family of novel adipokines, induce vascular relaxation through the adiponectin receptor-1/AMPK/eNOS/nitric oxide signaling pathway. *Arterioscler Thromb. Vasc. Biol.* **31**, 2616–2623 (2011).
23. Wong, G. W. et al. Molecular, biochemical and functional characterizations of Clq/TNF family members: adipose-tissue-selective expression patterns, regulation by PPAR-gamma agonist, cysteine-mediated oligomerizations, combinatorial associations and metabolic functions. *Biochem J.* **416**, 161–177 (2008).
24. Yamauchi, T. et al. Cloning of adiponectin receptors that mediate antidiabetic metabolic effects. *Nature* **423**, 762–769 (2003).
25. Yamauchi, T. et al. Targeted disruption of AdipoR1 and AdipoR2 causes abrogation of adiponectin binding and metabolic actions. *Nat. Med.* **13**, 332–339 (2007).
26. Seldin, M. M., Tan, S. Y. & Wong, G. W. Metabolic function of the CTRP family of hormones. *Rev. Endocr. Metab. Disord.* **15**, 111–123 (2014).
27. Tang, Y. T. et al. PAQR proteins: a novel membrane receptor family defined by an ancient 7-transmembrane pass motif. *J. Mol. Evol.* **61**, 372–380 (2005).
28. Tanabe, H. et al. Crystal structures of the human adiponectin receptors. *Nature* **520**, 312–316 (2015).
29. Vasiliuskaite-Brooks, I. et al. Structural insights into adiponectin receptors suggest ceramidase activity. *Nature* **544**, 120–123 (2017).
30. Holland, W. L. et al. Receptor-mediated activation of ceramidase activity initiates the pleiotropic actions of adiponectin. *Nat. Med.* **17**, 55–63 (2011).
31. Vasiliuskaite-Brooks, I., Healey, R. D. & Granier, S. 7TM proteins are not necessarily GPCRs. *Mol. Cell Endocrinol.* **491**, 110397 (2019).
32. Holland, W. L. & Scherer, P. E. Structural biology: Receptors grease the metabolic wheels. *Nature* **544**, 42–44 (2017).
33. Vasiliuskaite-Brooks, I. et al. Structure of a human intramembrane ceramidase explains enzymatic dysfunction found in leukodystrophy. *Nat. Commun.* **9**, 5437 (2018).
34. Kahn, B. B., Alquier, T., Carling, D. & Hardie, D. G. AMP-activated protein kinase: ancient energy gauge provides clues to modern understanding of metabolism. *Cell Metab.* **1**, 15–25 (2005).
35. Kersten, S., Desvergne, B. & Wahli, W. Roles of PPARs in health and disease. *Nature* **405**, 421–424 (2000).
36. Yamauchi, T. et al. Adiponectin stimulates glucose utilization and fatty-acid oxidation by activating AMP-activated protein kinase. *Nat. Med.* **8**, 1288–1295 (2002).
37. Tomas, E. et al. Enhanced muscle fat oxidation and glucose transport by ACRP30 globular domain: acetyl-CoA carboxylase inhibition and AMP-activated protein kinase activation. *Proc. Natl Acad. Sci. USA* **99**, 16309–16313 (2002).
38. Rasmussen, M. S. et al. Adiponectin receptors in human adipose tissue: effects of obesity, weight loss, and fat depots. *Obes. (Silver Spring)* **14**, 28–35 (2006).
39. Okada-Iwabu, M. et al. A small-molecule AdipoR agonist for type 2 diabetes and short life in obesity. *Nature* **503**, 493–499 (2013).
40. Iwabu, M. et al. Adiponectin and AdipoR1 regulate PGC-1alpha and mitochondria by Ca(2+) and AMPK/SIRT1. *Nature* **464**, 1313–1319 (2010).
41. Okada-Iwabu, M., Iwabu, M., Ueki, K., Yamauchi, T. & Kadowaki, T. Perspective of small-molecule AdipoR Agonist For Type 2 Diabetes And Short Life In Obesity. *Diabetes Metab. J.* **39**, 363–372 (2015).
42. Iwabu, M., Okada-Iwabu, M., Yamauchi, T. & Kadowaki, T. Adiponectin/adiponectin receptor in disease and aging. *NPJ Aging Mech. Dis.* **1**, 15013 (2015).
43. Wu, Z. et al. Mechanisms controlling mitochondrial biogenesis and respiration through the thermogenic coactivator PGC-1. *Cell* **98**, 115–124 (1999).
44. Mootha, V. K. et al. Erralpha and Gabpa/b specify PGC-1alpha-dependent oxidative phosphorylation gene expression that is altered in diabetic muscle. *Proc. Natl Acad. Sci. USA* **101**, 6570–6575 (2004).
45. Shulman, G. I. Cellular mechanisms of insulin resistance. *J. Clin. Invest.* **106**, 171–176 (2000).
46. Berchtold, M. W., Brinkmeier, H. & Muntener, M. Calcium ion in skeletal muscle: its crucial role for muscle function, plasticity, and disease. *Physiol. Rev.* **80**, 1215–1265 (2000).
47. Meinild Lundby, A. K. et al. Exercise training increases skeletal muscle mitochondrial volume density by enlargement of existing mitochondria and not de novo biogenesis. *Acta Physiol. (Oxf)* **222**, <https://doi.org/10.1111/apha.12905> (2018).
48. Handschin, C. & Spiegelman, B. M. The role of exercise and PGC1alpha in inflammation and chronic disease. *Nature* **454**, 463–469 (2008).
49. Mootha, V. K. et al. PGC-1alpha-responsive genes involved in oxidative phosphorylation are coordinately downregulated in human diabetes. *Nat. Genet.* **34**, 267–273 (2003).
50. Canto, C. et al. AMPK regulates energy expenditure by modulating NAD+ metabolism and SIRT1 activity. *Nature* **458**, 1056–1060 (2009).
51. Paffenbarger, R. S. Jr. et al. The association of changes in physical-activity level and other lifestyle characteristics with mortality among men. *N. Engl. J. Med.* **328**, 538–545 (1993).
52. Lindgren, A. et al. Adiponectin receptor 2 deficiency results in reduced atherosclerosis in the brachiocephalic artery in apolipoprotein E deficient mice. *PLoS ONE* **8**, e80330 (2013).
53. Maeda, N. et al. Diet-induced insulin resistance in mice lacking adiponectin/ACRP30. *Nat. Med.* **8**, 731–737 (2002).
54. Kubota, N. et al. Disruption of adiponectin causes insulin resistance and neointimal formation. *J. Biol. Chem.* **277**, 25863–25866 (2002).
55. Nawrocki, A. R. et al. Mice lacking adiponectin show decreased hepatic insulin sensitivity and reduced responsiveness to peroxisome proliferator-activated receptor gamma agonists. *J. Biol. Chem.* **281**, 2654–2660 (2006).
56. Olson, E. N., Arnold, H. H., Rigby, P. W. & Wold, B. J. Know your neighbors: three phenotypes in null mutants of the myogenic bHLH gene MRF4. *Cell* **85**, 1–4 (1996).
57. Ramirez-Solis, R., Zheng, H., Whiting, J., Krumlauf, R. & Bradley, A. Hoxb-4 (Hox-2.6) mutant mice show homeotic transformation of a cervical vertebra and defects in the closure of the sternal rudiments. *Cell* **73**, 279–294 (1993).
58. Fiering, S. et al. Targeted deletion of 5'HS2 of the murine beta-globin LCR reveals that it is not essential for proper regulation of the beta-globin locus. *Genes Dev.* **9**, 2203–2213 (1995).
59. Matsuzawa, Y. Pathophysiology and molecular mechanisms of visceral fat syndrome: the Japanese experience. *Diabetes Metab. Rev.* **13**, 3–13 (1997).
60. Reaven, G. Insulin resistance and coronary heart disease in nondiabetic individuals. *Arterioscler Thromb. Vasc. Biol.* **32**, 1754–1759 (2012).
61. Calle, E. E., Rodriguez, C., Walker-Thurmond, K. & Thun, M. J. Overweight, obesity, and mortality from cancer in a prospectively studied cohort of U.S. adults. *N. Engl. J. Med.* **348**, 1625–1638 (2003).
62. Holland, W. L. & Scherer, P. E. Cell Biology. Ronning after the adiponectin receptors. *Science* **342**, 1460–1461 (2013).
63. Rosen, E. D. & Spiegelman, B. M. What we talk about when we talk about fat. *Cell* **156**, 20–44 (2014).
64. Kubota, N. et al. Pioglitazone ameliorates insulin resistance and diabetes by both adiponectin-dependent and -independent pathways. *J. Biol. Chem.* **281**, 8748–8755 (2006).
65. Kamei, N. et al. Overexpression of monocyte chemoattractant protein-1 in adipose tissues causes macrophage recruitment and insulin resistance. *J. Biol. Chem.* **281**, 26602–26614 (2006).
66. Minokoshi, Y. et al. Leptin stimulates fatty-acid oxidation by activating AMP-activated protein kinase. *Nature* **415**, 339–343 (2002).
67. Tsao, T. S., Murrey, H. E., Hug, C., Lee, D. H. & Lodish, H. F. Oligomerization state-dependent activation of NF-kappa B signaling pathway by adipocyte

- complement-related protein of 30 kDa (Acrp30). *J. Biol. Chem.* **277**, 29359–29362 (2002).
68. Woods, A., Salt, I., Scott, J., Hardie, D. G. & Carling, D. The alpha1 and alpha2 isoforms of the AMP-activated protein kinase have similar activities in rat liver but exhibit differences in substrate specificity in vitro. *FEBS Lett.* **397**, 347–351 (1996).
69. Hayashi, T. et al. Metabolic stress and altered glucose transport: activation of AMP-activated protein kinase as a unifying coupling mechanism. *Diabetes* **49**, 527–531 (2000).
70. Civitarese, A. E. et al. Role of adiponectin in human skeletal muscle bioenergetics. *Cell Metab.* **4**, 75–87 (2006).
71. Heilbronn, L. K. et al. Glucose tolerance and skeletal muscle gene expression in response to alternate day fasting. *Obes. Res.* **13**, 574–581 (2005).
72. Molina, A. J. et al. Skeletal muscle mitochondrial content, oxidative capacity, and Mfn2 Expression Are reduced in older patients with heart failure and preserved ejection fraction and are related to exercise intolerance. *JACC Heart Fail* **4**, 636–645 (2016).

Acknowledgements

The authors thank research group members department of diabetes and metabolic diseases, graduate school of medicine, The University of Tokyo, for technical assistance, support with in vivo studies and for experimental help. This work was supported by JSPS KAKENHI Grant Numbers JP18K10988 (M.I.), JP16K15487, JP26293216, JP19K11639 (M.O.-I.), JP26000012, JP19H01052 (T.Kadowaki), by the Translational Research Network Program (AMED) (M.O.-I.) and by JST, PRESTO (JPMJPR13MF) (M.I.).

Author contributions

M.I., M.O.-I., T.Y., and T. Kadowaki designed the research. M.I. and M.O.-I. performed all experiments. N.O. and K.M. performed in vitro and in vivo experiments. T. Kobori,

S.O., and Y.K. supported in vivo experiments. M.I., M.O.-I., H.T., S.Y., T.Y., and T.Kadowaki wrote the main manuscript. All authors reviewed the manuscript.

Competing interests

The authors declare no competing interests.

Additional information

Supplementary information is available for this paper at <https://doi.org/10.1038/s42003-020-01579-9>.

Correspondence and requests for materials should be addressed to M.O.-I., T.Y. or T.K.

Reprints and permission information is available at <http://www.nature.com/reprints>

Publisher's note Springer Nature remains neutral with regard to jurisdictional claims in published maps and institutional affiliations.



Open Access This article is licensed under a Creative Commons Attribution 4.0 International License, which permits use, sharing, adaptation, distribution and reproduction in any medium or format, as long as you give appropriate credit to the original author(s) and the source, provide a link to the Creative Commons license, and indicate if changes were made. The images or other third party material in this article are included in the article's Creative Commons license, unless indicated otherwise in a credit line to the material. If material is not included in the article's Creative Commons license and your intended use is not permitted by statutory regulation or exceeds the permitted use, you will need to obtain permission directly from the copyright holder. To view a copy of this license, visit <http://creativecommons.org/licenses/by/4.0/>.

© The Author(s) 2021